Published in final edited form as:
*Nature*. 2012 November 29; 491(7426): 761–764. doi:10.1038/nature11587.

# A Map of Visual Space in the Primate Entorhinal Cortex

**Nathaniel J Killian**[1,2], **Michael J Jutras**[1], and **Elizabeth A Buffalo**[1,3]

Nathaniel J Killian: njkillian@gatech.edu; Michael J Jutras: mjutras@emory.edu; Elizabeth A Buffalo: elizabeth.buffalo@emory.edu

[1]Yerkes National Primate Research Center, 954 Gatewood Road, Atlanta, GA 30329, USA

[2]Wallace H. Coulter Department of Biomedical Engineering at Georgia Tech and Emory University, 313 Ferst Dr, Atlanta, GA, 30332, USA

[3]Department of Neurology, Emory University School of Medicine, 1440 Clifton Road, Atlanta, GA, 30322, USA

## Abstract

Place-modulated activity among neurons in the hippocampal formation presents a means to organize contextual information in the service of memory formation and recall[1,2]. One particular spatial representation, that of grid cells, has been observed in the entorhinal cortex (EC) of rats and bats[3–5], but has yet to be described in single units in primates. Here, we examined spatial representations in the EC of head-fixed monkeys performing a free-viewing visual memory task[6,7]. Individual neurons were identified in the primate EC that emitted action potentials when the monkey fixated multiple discrete locations in the visual field across the presentation of up to hundreds of novel images. These firing fields possess spatial periodicity similar to a triangular tiling with a corresponding well-defined hexagonal structure in the spatial autocorrelation. Further, these neurons demonstrated theta-band oscillatory activity and changing spatial scale as a function of distance from the rhinal sulcus, which is consistent with previous findings in rodents[4,8–10]. These spatial representations may provide a framework to anchor the encoding of stimulus content in a complex visual scene. Together, our results provide a direct demonstration of grid cells in the primate and suggest that EC neurons encode space during visual exploration, even without locomotion.

### Keywords

spatial representation; primate; medial temporal lobe; entorhinal cortex; hippocampus; grid cells; border cells; memory

The primate hippocampus has been shown to represent both egocentric spatial information, with cells responding to self-motion and head-direction information, as well as allocentric spatial information, with cells firing spikes in response to place 'out there'[1,11–14]. The presence of allocentric spatial view cells, analogous to rodent place cells, suggests that the primate entorhinal cortex (EC) may also represent space independent of the position of the

Correspondence and requests: for materials should be addressed to E.A.B. (elizabeth.buffalo@emory.edu).

Supplementary Information: is linked to the online version of the paper at www.nature.com/nature.

**Author contributions:** E.A.B. and N.J.K. designed the research, N.J.K. collected the data from the EC, M.J.J. collected data from the HPC, N.J.K. performed the analyses, and N.J.K. and E.A.B. wrote the paper.



The authors declare no competing financial interests.

Readers are welcome to comment on the online version of this article at www.nature.com/nature.

animal. Indeed, the nonretinocentric, bilateral receptive fields of primate EC neurons allow for the possibility of regular and allocentric spatial firing within the EC[15]. Furthermore, a recent study has provided evidence for grid cells based on human neuronal population responses in the EC that are periodic with respect to position in virtual space[16]. To examine spatial representations in the primate hippocampal formation, we recorded the activity of 342 neurons from the EC and hippocampus of three monkeys performing a free-viewing visual recognition memory task, the Visual Preferential Looking Task (VPLT)[6,7]. Novel images were each presented twice on a computer monitor with a fixed reference frame and gaze location was recorded simultaneously with neuronal data. Images consisted of photographs that contained a wide variety of elements including abstract art, animals, landscapes, and people, and the monkeys explored the static images with a dynamic sequence of fixations (Fig. 1a). On average, EC neurons gave enhanced responses to stimulus presentation and many demonstrated a reduced firing rate for repeat presentations, consistent with previous findings of match-suppression (Fig. 2)[15]. Neurons in the hippocampus exhibited a more diverse range of suppressed and excited visual and recognition responses[6]. All of these responses were contained within the analyzed data; we included data segments in the analyses if and only if the monkey was actively exploring an image on the screen (prestimulus fixation periods and viewing outside of the image bounds were not included).

In the rat EC, grid cells are found exclusively in the medial EC (MEC). Spatial and visual input to the EC is topographically organized such that spatial information reaches the MEC via input from the postrhinal (TF/TH in primates) cortex, while visual object information reaches lateral EC (LEC) via the perirhinal cortex[17]. In monkeys, roughly the posterior half of the EC receives visuospatial information from parahippocampal cortex (TF/TH), retrosplenial cortex, and presubiculum, while the anterior half receives visual object information from the perirhinal cortex[18]. Projections from EC to the hippocampus also have a similar anatomical organization in rats and monkeys, but the anatomical axes are oriented differently. Anterior EC in the monkey and LEC in the rat project to the region around the border between CA1 and subiculum, while posterior EC in the monkey and MEC in the rat project to proximal CA1 and distal subiculum[19]. Based on the topography of these inputs, we would expect the rat MEC and LEC to correspond to posterior and anterior EC, respectively, in monkeys.

The spatial firing fields of grid cells can be thought of as representing the nodes of a triangular grid, and it follows that the spatial autocorrelation of the firing rate map should have a well-defined hexagon surrounding a central peak. A gridness score has been used to quantify the strength of 60-degree rotational symmetry that leads to this hexagonal structure (Supplementary Fig. 1)[10,20]. The gridness of all recorded units was evaluated and surrogate data were used to determine significant gridness scores. Grid cells were classified as those having a gridness score above the 95$^{th}$ percentile of the scores for 100 time-shifted permutations of the spike timings (Fig. 1b, e). The number of grid cells identified in the posterior EC, (23/193, 11.9%) was significantly greater than that expected by chance ($P < 0.0001$, $\chi^2(19.4,1)$) (Fig. 1b, c; see also Supplementary Figs 2a and 3). Importantly, the spatial density of gaze location did not produce high gridness scores (Supplementary Fig. 2b), and across the population, the grid scores for EC grid cells were consistently higher than grid scores calculated for eye movements ($P < 1\times10^{-8}$, Wilcoxon rank-sum test; Supplementary Fig. 2b). Because these analyses were computed across presentations of multiple complex stimuli, these data suggest that the grid cell representation is not specific to stimulus content. In order to explicitly address this, we examined the reliability of these representations by comparing the rate maps generated from the first and second halves of each session. There was a significant positive correlation between these firing rate maps

across the population of grid cells ($P < 1\times10^{-5}$, $n = 23$, signed rank test), which suggests that these representations are stable and stimulus-independent (see Supplementary Fig. 4).

The proportion of grid cells identified in the hippocampus (4/119, 3.4%) was not significantly different from chance ($P = 0.41$, $\chi^2(0.67,1)$) and was significantly less than the number of EC grid cells ($P = 0.009$, $\chi^2(6.82,1)$) (Fig. 1c). An important caveat is that our hippocampal recordings were all taken from the anterior hippocampus[7], which is presumably comparable to the temporal hippocampus in rats, containing cells with larger place fields than in septal regions. Accordingly, it is difficult to compare the scale of the spatial representations between the EC and HPC with the present data.

We also found a significant population of neurons in the EC, but not the HPC, with increased firing rate near the edges of the stimuli, quantified using a border score as described in [5] (Fig. 1c, e) (EC: $P = 0.0058$, $\chi^2(7.61,1)$, 18/193 (9.3%); HPC: $P = 0.1995$, $\chi^2(1.65,1)$, 9/119 (7.6%); see Supplementary Information for a detailed description of methods). The presence of cells that represent spatial locations relative to the stimulus bounds independent of stimulus content would suggest that representations of objects within an environment may be anchored to a consistent framework, with the stimulus bounds serving as landmarks. However, it is possible that these neurons simply have oblong view fields near one or more edges of the image presentation region. This would need to be examined in future studies with changing image frames.

In the rat and bat EC, grid cells increase in field spacing in the dorsomedial to ventrolateral direction, with distance from the border of the MEC with the postrhinal cortex[3,4]. This gradient mirrors the increase in the size of hippocampal place fields along the dorsoventral axis[21], to which the MEC provides input in a topographical manner[17,22]. In the monkey, cells located in lateral EC (close to the rhinal sulcus) project to posterior levels of the hippocampus while cells located in medial EC project to more anterior levels of the hippocampus[19,22]. In the present study, firing field spacing was significantly correlated with distance from the rhinal sulcus for each monkey and for both monkeys taken together (MP: $\rho = 0.671$, $P = 0.024$; TT: $\rho = 0.665$, $P = 0.026$; both monkeys: $\rho = 0.567$, $P = 0.006$) (Fig. 1d; see also Supplementary Figure 5).

Along with spatial representations, we also examined neuronal responses in the EC that might underlie recognition memory. Consistent with the input from perirhinal cortex to anterior EC, we found that neurons in anterior EC demonstrated stronger visual and memory responses than did neurons in posterior EC. Specifically, a larger proportion of neurons responsive to visual stimuli were found at more anterior locations ($P = 0.0062$, $\chi^2(7.5,1)$), and among these visually responsive neurons, a larger proportion demonstrated a reduction in firing rate for repeated stimuli, i.e., “match-suppression”, at more anterior locations ($P = 6.67\times10^{-9}$, $\chi^2(33.63,1)$) (Supplementary Fig. 6). Furthermore, among the neurons displaying significant match-suppression, the relative decrease in firing rate for repeat presentations was greater at more anterior locations (Fig. 2). Interestingly, the recognition memory and spatial representations were somewhat independent of each other; at more anterior recording locations, grid cells were more likely to also exhibit a memory response, with a firing rate reduction magnitude in line with the rest of the population of cells ($P = 0.0034$, $\chi^2(8.55,1)$). However, there was a gradual decline in the percentage of grid cells at more anterior locations, and no grid cells were found in any of 3 separate penetrations in front of the posterior 50% of the EC, suggesting a functional border between posterior and anterior EC. Because most of our recordings were in the posterior EC, an important target of future studies will be to further characterize responses throughout the anterior EC.

EC layers were classified using current-source density estimates (see Supplementary Methods). Grid cells were found at an approximately equal frequency across both superficial and deep layers (14/125 in superficial layers and 9/68 in deep layers), suggesting that grid cells play a role in processing both input to and output from the hippocampus. Because many grid cells in layers deeper than layer II are modulated by head direction in rodents, it is possible that recording with the monkey's head positioned in variable directions would increase these percentages. In addition, the physical restriction of using dorsal to ventral penetrations precludes higher sampling of the thin layer II that possesses the largest percentage of grid cells in rodents.

Because theta-band modulation is critical to certain models that describe the generation of grid cells[23], we next examined theta-band oscillatory activity in individual EC grid cells and in the simultaneously recorded local field potential (LFP) on an adjacent electrode. We found that the EC exhibits intermittent bouts of theta oscillations similar to the theta bouts previously described in the primate hippocampus (Fig. 3a)[24,25]. These bouts, detected during blocks of image presentations, had a mean duration of 1.09 ± 0.86 s and a mean inter-bout interval of 0.95 ± 0.94 s (mean ± s.d.). We also found that across the recording session, the grid cells were phase-locked to the trough of the LFP theta (Fig. 3b) and the spike trains of 13 of 23 grid cells (57%) were theta-modulated (Fig. 3c), consistent with findings in rodents[26,27]. Theta-modulation and phase-locking were not limited to grid cells but were observed in the population of EC and HPC neurons as a whole (Supplementary Fig. 7c, d). During image viewing, saccades were made at a median rate of 3.92 Hz (Fig. 3d), but the precise timing of saccades was not theta modulated across the session, suggesting that the theta modulation of grid cells was not due to rhythmicity in eye movements (Fig. 3e). Firing rate maps for bout periods were correlated with non-bout periods ($P < 0.01$, Wilcoxon signed-rank test) and we did not find a significant difference in the grid pattern between bouts and non-bouts (Supplementary Fig. 8). Future experiments involving disruption of theta would aid in understanding the relationship between primate theta and spatial firing patterns[9,10]. Importantly, the present data demonstrate theta-band modulation among EC grid cells, even in a species with non-continuous theta. This information is critical for informing computational models and increasing our understanding of the generation of these spatial representations[23,28].

Taken together, these data provide evidence for grid cells in the primate entorhinal cortex. These spatial responses are similar in many respects to grid cells that have been described previously in the rat and bat during locomotion, but were identified with a distinct method of sampling the environment, i.e., visual exploration through eye movements. These results suggest that spatial representations in primates can arise during visual exploration at a distance, without requiring an actual visit to that place. Accordingly, these data suggest that theories of spatial representation in the context of navigation could be applied to visual exploration. Because these experiments were performed with the monkey's head and the visual stimulus in a given, fixed position, we are not able to identify whether these grid cells represent allocentric or egocentric spatial locations. Notably, although grid-cell spiking was theta-modulated, we found significant evidence for grid cells in the absence of continuous theta-band oscillations in the LFP. These data suggest that current models of grid cells based on interactions of oscillations will need to be adapted to account for both intermittent theta and exploration through saccadic movements. One possibility is that saccades produce a theta-band phase shift in the LFP. This could modulate the theta-band frequency in a way that might be comparable to the modulation in frequency that occurs through movement velocity in rodents. It is also likely that an optimal model will include aspects of current oscillatory interaction and network attractor models[29]. These results provide a potential challenge to the view that grid cells support path integration by combining self-motion and environment cues[4]; however, it will be important to determine whether corollary discharge

signals that enable the monitoring of eye movement commands might contribute significantly to the generation of grid fields[30]. It is possible that the spatial representations identified here reflect an integration of environmental context and the magnitude of eye movements, but this will need to be carefully examined in future experiments.

## METHODS SUMMARY

In each VPLT session, 200 novel images were each presented twice on a computer monitor in a randomly interleaved fashion within 11×11 degrees visual angle (dva) in the center of the monitor. Monkeys were head-fixed and sitting in a chair with the center of the monitor aligned to their neutral eye position. An image was removed after the monkey looked outside the image bounds or after 5 seconds. In a second version of the task that was used to record from 7 EC units, images covered the entire viewable region of the monitor ($33.\bar{3} \times 25$ dva). In this version, each of 36 novel scenes was shown twice and a total of 10 seconds of visual exploration was required for each presentation. Gaze location was recorded with an infrared eye-tracking system (ISCAN, Inc.). We recorded spikes (250–8000 Hz) and LFPs (0.7–170 Hz) from the EC with a laminar electrode array mounted on a tungsten microelectrode (12-site, 150 μm spacing; FHC, Inc.). Rate maps were computed with a Gaussian smoothing procedure[27]. Gridness scores and border scores were calculated using standard equations and significance was evaluated with a standard shuffling procedure[5,27]. Theta-band bouts in the LFP were detected by statistically analyzing the power spectrum over time[25]. Theta-band modulation of grid cells was analyzed with a standard autocorrelogram power spectrum metric, the theta index[27]. All experiments were carried out in accordance with protocols approved by the Emory University Institutional Animal Care and Use Committee.

## Supplementary Material

Refer to Web version on PubMed Central for supplementary material.

## Acknowledgments

We thank S. Potter, C. Erickson, J. Manns, and M. Meister for comments on the manuscript, and M. Tompkins and D. Solyst for assistance with experiments. This project was funded by the National Institute of Mental Health, R01MH093807 (E.A.B.), R01MH080007 (E.A.B.), MH082559 (M.J.J.), the National Center for Research Resources P51RR165, and is currently supported by the Office of Research Infrastructure Programs/OD P51OD11132. N.J.K. was supported by the NSF IGERT program (DGE-0333411).

## References

1. Ekstrom AD, et al. Cellular networks underlying human spatial navigation. Nature. 2003; 425:184–8. [PubMed: 12968182]
2. Moser EI, Kropff E, Moser MB. Place cells, grid cells, and the brain's spatial representation system. Annu Rev Neurosci. 2008; 31:69–89. [PubMed: 18284371]
3. Yartsev MM, Witter MP, Ulanovsky N. Grid cells without theta oscillations in the entorhinal cortex of bats. Nature. 2011; 479:103–107. [PubMed: 22051680]
4. Hafting T, Fyhn M, Molden S, Moser MB, Moser EI. Microstructure of a spatial map in the entorhinal cortex. Nature. 2005; 436:801–6. [PubMed: 15965463]
5. Solstad T, Boccara CN, Kropff E, Moser MB, Moser EI. Representation of geometric borders in the entorhinal cortex. Science. 2008; 322:1865–8. [PubMed: 19095945]
6. Jutras MJ, Buffalo EA. Recognition memory signals in the macaque hippocampus. Proc Natl Acad Sci U S A. 2010; 107:401–6. [PubMed: 20018683]
7. Jutras MJ, Fries P, Buffalo EA. Gamma-band synchronization in the macaque hippocampus and memory formation. J Neurosci. 2009; 29:12521–31. [PubMed: 19812327]

8. Hafting T, Fyhn M, Bonnevie T, Moser MB, Moser EI. Hippocampus-independent phase precession in entorhinal grid cells. Nature. 2008; 453:1248–52. [PubMed: 18480753]
9. Koenig J, Linder AN, Leutgeb JK, Leutgeb S. The spatial periodicity of grid cells is not sustained during reduced theta oscillations. Science. 2011; 332:592–5. [PubMed: 21527713]
10. Brandon MP, et al. Reduction of theta rhythm dissociates grid cell spatial periodicity from directional tuning. Science. 2011; 332:595–9. [PubMed: 21527714]
11. Rolls ET. Spatial view cells and the representation of place in the primate hippocampus. Hippocampus. 1999; 9:467–80. [PubMed: 10495028]
12. Tamura R, Ono T, Fukuda M, Nakamura K. Spatial responsiveness of monkey hippocampal neurons to various visual and auditory stimuli. Hippocampus. 1992; 2:307–22. [PubMed: 1308190]
13. Ono T, Nakamura K, Nishijo H, Eifuku S. Monkey hippocampal neurons related to spatial and nonspatial functions. J Neurophysiol. 1993; 70:1516–1529. [PubMed: 8283212]
14. Robertson RG, Rolls ET, Georges-François P, Panzeri S. Head direction cells in the primate pre-subiculum. Hippocampus. 1999; 9:206–19. [PubMed: 10401637]
15. Suzuki WA, Miller EK, Desimone R. Object and place memory in the macaque entorhinal cortex. J Neurophysiol. 1997; 78:1062–81. [PubMed: 9307135]
16. Doeller CF, Barry C, Burgess N. Evidence for grid cells in a human memory network. Nature. 2010; 463:657–661. [PubMed: 20090680]
17. Witter MP, Wouterlood FG, Naber PA, Van Haeften T. Anatomical organization of the parahippocampal-hippocampal network. Ann N Y Acad Sci. 2000; 911:1–24. [PubMed: 10911864]
18. Insausti R, Amaral DG. Entorhinal cortex of the monkey: IV. Topographical and laminar organization of cortical afferents. J Comp Neurol. 2008; 509:608–41. [PubMed: 18551518]
19. Witter MP, Amaral DG. Entorhinal cortex of the monkey: V. Projections to the dentate gyrus, hippocampus, and subicular complex. J Comp Neurol. 1991; 307:437–59. [PubMed: 1713237]
20. Sargolini F, et al. Conjunctive representation of position, direction, and velocity in entorhinal cortex. Science. 2006; 312:758–62. [PubMed: 16675704]
21. Kjelstrup KB, et al. Finite scale of spatial representation in the hippocampus. Science (New York, NY). 2008; 321:140–3.
22. Canto CB, Wouterlood FG, Witter MP. What does the anatomical organization of the entorhinal cortex tell us? Neural Plast. 2008; 2008:381243. [PubMed: 18769556]
23. Burgess N, Barry C, Keefe JO. An Oscillatory Interference Model of Grid Cell Firing. Hippocampus. 2007; 812:801–812. [PubMed: 17598147]
24. Stewart M, Fox SE. Hippocampal theta activity in monkeys. Brain Res. 1991; 538:59–63. [PubMed: 2018932]
25. Ekstrom AD, et al. Human hippocampal theta activity during virtual navigation. Hippocampus. 2005; 15:881–9. [PubMed: 16114040]
26. Mizuseki K, Sirota A, Pastalkova E, Buzsáki G. Theta oscillations provide temporal windows for local circuit computation in the entorhinal-hippocampal loop. Neuron. 2009; 64:267–80. [PubMed: 19874793]
27. Langston RF, et al. Development of the spatial representation system in the rat. Science. 2010; 328:1576–80. [PubMed: 20558721]
28. Burgess N, O'Keefe J. Models of place and grid cell firing and theta rhythmicity. Curr Opin Neurobiol. 2011; 21:734–44. [PubMed: 21820895]
29. McNaughton BL, Battaglia FP, Jensen O, Moser EI, Moser MB. Path integration and the neural basis of the "cognitive map". Nature Rev Neurosci. 2006; 7:663–78. [PubMed: 16858394]
30. Sommer MA, Wurtz RH. A pathway in primate brain for internal monitoring of movements. Science. 2002; 296:1480–2. [PubMed: 12029137]

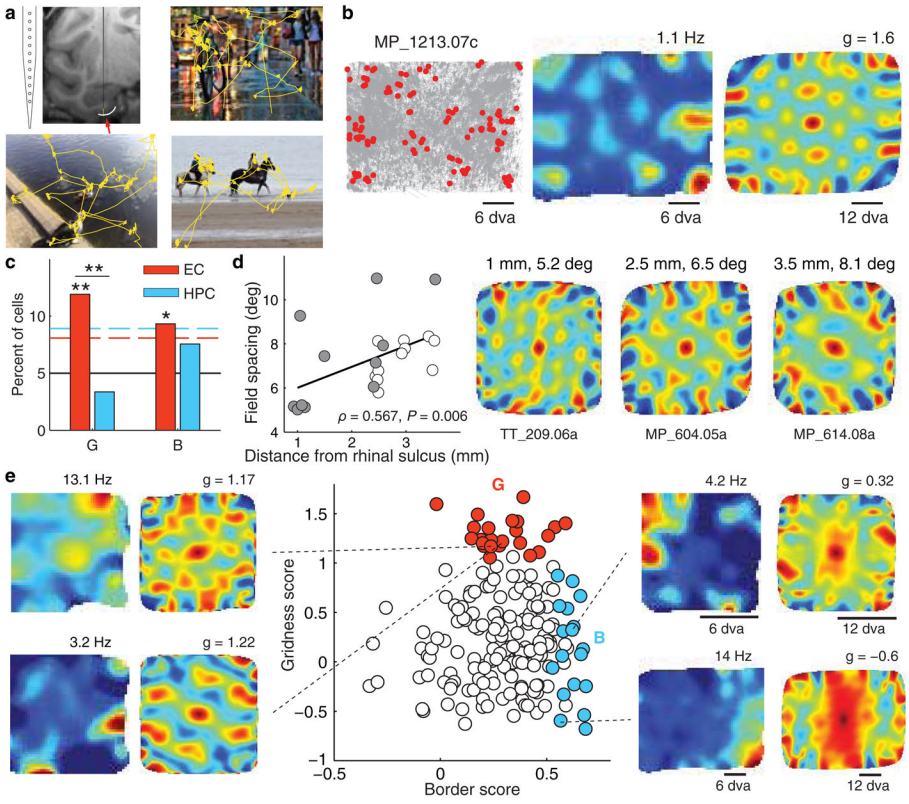


**Figure 1. Spatial representation in the primate entorhinal cortex**

**a.** Recordings were performed using a linear electrode array placed in the entorhinal cortex (red arrow). Three example 10-second scan paths are shown in yellow. **b.** An example of an entorhinal grid cell. Left: plots of eye position (gray) and spikes (red) reveal non-uniform spatial density of spiking. For clarity, only spikes corresponding to locations of firing rate above half of the mean rate were plotted. Monkey name and unit number are indicated by the characters at the top. Middle: spatial firing rate maps show multiple distinct firing fields. The maximum of the rate map (red) is given at the top. Right: the spatial periodicity of the firing fields is seen with spatial autocorrelations. The color scale limits are ±1 (blue-red), the maximum correlation magnitude, with green being 0 correlation. g = gridness score, dva = degrees of visual angle. **c.** Percentages of cells in the EC and HPC with a significantly high gridness score (G), or border score (B). The black line shows the 5% chance level, the dashed lines represent the 95% confidence level; $*P < 0.05$, $**P < 0.01$. **d.** Grid cell spacing increased with distance from the rhinal sulcus, consistent with a dorsal-ventral gradient in rodents and bats. Open and closed circles identify the grid cells from each of the two monkeys. Right: autocorrelations for representative grid cells recorded at different locations medial to the rhinal sulcus. **e.** Gridness and border scores are plotted for all cells recorded in the posterior EC ($n = 193$; red: cells with significant gridness scores, $n = 23$; blue: cells with significant border scores, $n = 18$).

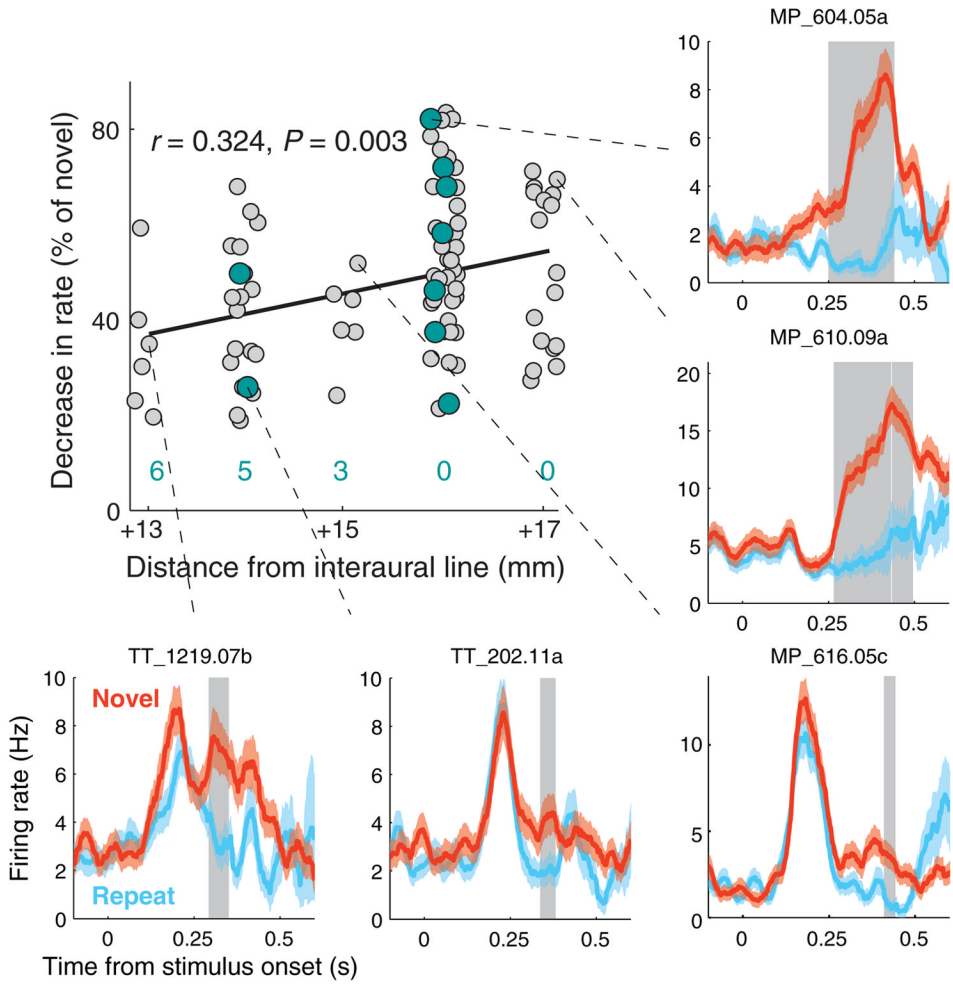


**Figure 2. Recognition memory and conjunctive grid-memory cells**

The strength of the memory response (% decrease in rate for repeated stimuli) increased in more anterior recording locations ($n = 85$ cells with a significant recognition memory response). Grid cells (teal) were more likely to show a recognition memory response at more anterior locations (the number of grid cells without a significant memory response at each location is shown in teal). Neuronal responses to novel and repeat presentations are shown for some representative neurons (mean ± s.e.m.). Gray shading indicates a time region of significant decrease in firing rate for repeat presentations ($P < 0.025$, see Supplementary Methods).

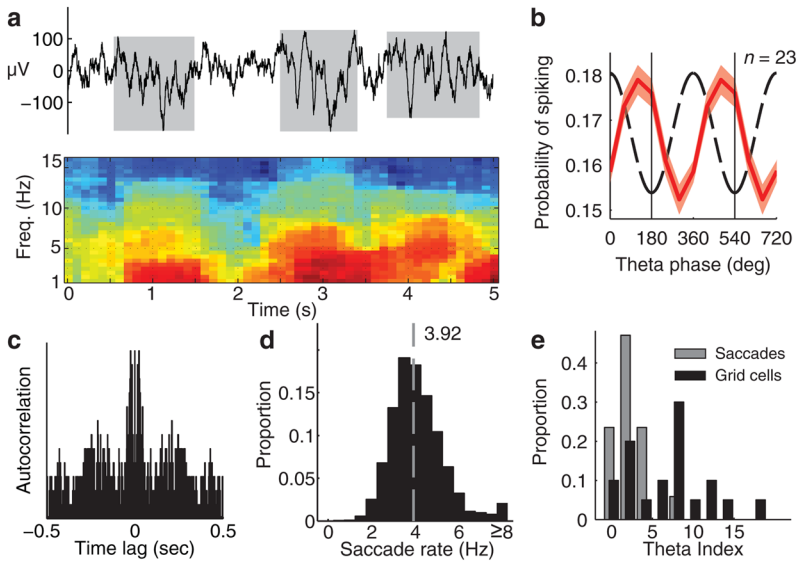


**Figure 3. Theta bouts and theta modulation of grid cells**

**a.** Top: 5 second raw LFP trace with theta (3–12 Hz) bouts indicated in gray. Bottom: spectrogram showing the power (dB) of the top LFP trace. **b.** Grid cells were phase-locked to LFP theta (60-degree bins, red curve: mean ± s.e.m., dashed curve: prototype theta oscillation, two cycles are shown). **c.** Autocorrelation showing theta modulation of the spike train of a grid cell (theta index = 11.2 at 4.2 Hz). **d.** Histogram of the saccade rate during image viewings in 19 sessions (4.16 ± 1.49 Hz, mean ± s. d.., dashed gray line = median, 3.92). **e.** Saccade times ($n = 17$) resulted in lower theta indices than the grid cell spike trains ($n = 20$) ($P < 0.01$, $n = 15$, Wilcoxon rank-sum test).